SolarPACES 2022, 28th International Conference on Concentrating Solar Power and Chemical Energy Systems
Thermal Energy Storage Materials, Media, and Systems
https://doi.org/10.52825/solarpaces.v1i.643

Published: 05 Jan. 2024

Modeling Microwave Heating of Molten Salt for Thermal Storage Systems

Cristobal Valverde[1][https://orcid.org/0000-0002-1930-9476], Margarita M. Rodriguez-Garcia[1][https://orcid.org/0000-0002-0271-108X], and Esther Rojas[2][https://orcid.org/0000-0001-5881-5331]

[1] Plataforma Solar de Almería, Spain

[2] Ciemat-PSA, Spain

Abstract. With the aim of affordably storing energy produced by photovoltaic and wind power plants, Power-to-heat-to-power (or Carnot batteries) are proposed as an outstanding system capable of transforming this energy into heat through existing commercial thermal storage systems for thermosolar plants, and again produce electricity by connecting these storage systems to available power blocks that can come from dismantled carbon plants or any other such as gas plants, or even nuclear. On this basis, microwave heating is studied as feasible to store energy in molten solar salt: 60%w $NaNO_3$, 40%w KNO_3. This study is expected to provide some key points for the design of microwave systems for molten solar salt, analysing different simulated cases with numerical modeling: continuous flow microwave heating in an elliptical cavity with different flow rates – 1 l/min and 1.6 l/min – and different positions of the fluid carrier tube, and in a microwave oven with helical tubes.

Keywords: Molten Solar Salt, Continuous Flow Microwave, Numerical Modeling

1. Introduction

The current electricity generation system has photovoltaic and wind power plants that do not produce at their maximum capacity when there is a large energy resource due to low demand at the time [1]. In order to get the best performance of these plants, Power to Heat to Power storage units, P2H2P or Carnot batteries, result some of the most outstanding solutions capable of producing electricity regardless of whether the energy resource is available or not. The aim is to use the existing commercial storage systems in CSP power plants, which provide large storage capacities – currently up to 2 $GW_e\,h$-, at low cost – between 20 and 50 $€/kW_e\,h$ - whose reliability and good performance have been widely proved [2], to harness energy by heating solar salt as a storage medium and then releasing the stored energy via existing power blocks and grid connections from dismantled coal power plants [3, 4].

The most common way to heat solar salt is by the Joule effect through electric heat exchangers whose efficiency depends on the effectiveness of the convection heat transfer, which may be a problem in the case of solar salt due to its poor heat conductivity [5]. In contrast, microwave irradiation penetrates the material directly causing volumetric heating and reducing the required time for it. Consequently, the use of microwaves for heating purposes is found in many industrial applications such as food industry, medical applications or chemistry [6, 7].

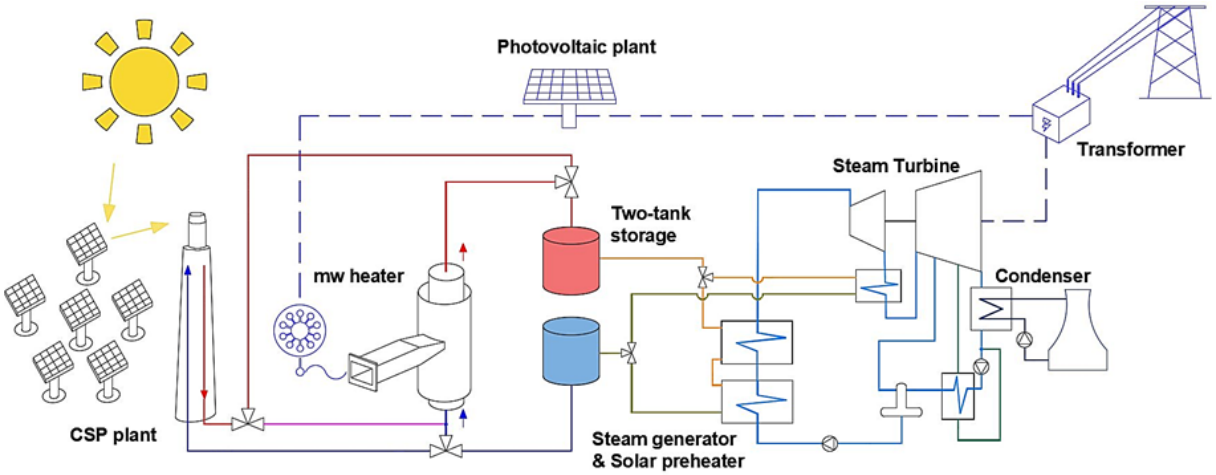

Figure 1. Diagram of a hybrid solar thermal and photovoltaic power plant with storage for both sources, using microwaves for the storage of photovoltaic electrical energy [8].

Modeling the microwave heating process is one of the most important activities to predict the temperature evolution within the processed material and to optimize the heating by reducing the non-uniform temperature distribution that highly depends on the geometrical configuration of the microwave unit and the dielectric properties of the materials [9-11]. These factors make it difficult to control the heating process, so numerical modeling has been widely used, for example to study emerging technologies such as continuous flow focused microwave systems in resonant cavities or the performance of helical tubes in a continuous flow microwave system [12, 13].

Based on these last two works [12, 13] and having measured the dielectric properties of the solar salt [5], the current study is dedicated to simulate the heating of this storage medium in an elliptical single mode cavity, at different flow rates – 1 l/min and 1.6 l/min – and at different positions of the carrier tube in the cavity. In addition, a more complex case in a multimode cavity crossed by a helical tube is simulated to study the effect of this special geometry of the tube. This is intended to provide some clues to understand the interaction of the solar salt with microwaves and provide the first steps to design a cost-effective and efficient system for microwave solar salt heating.

2. Material and methods

2.1 Dielectric properties of solar salt

Parameters such as dielectric constant (ε'), dielectric loss factor (ε''), and the derived loss tangent $(\tan\delta)$, equation (1), and penetration depth (Dp), equation (2), determine the feasibility of the material to be heated by microwaves. Thus, a material with a very large penetration depth, for example quartz glass whose penetration depth is about 160 m, is considered a transparent material as the energy is poorly absorbed, whereas high dielectric loss materials, and therefore, with low penetration depth, act as microwave reflectors [14].

$$\tan\delta = \frac{\varepsilon''}{\varepsilon'} \qquad (1)$$

$$Dp = \frac{\lambda_0}{\pi\sqrt{2\varepsilon'}\sqrt{\sqrt{(1+(\tan\delta)^2)}-1}} \qquad (2)$$

The method for determining the dielectric properties of solar salt makes use of a dual-mode-cavity where heating and measuring is performed simultaneously with two different microwave sources and a cross-coupling filter that provides a high isolation between both cavity modes. The relative complex permittivity is calculated by an enhanced cavity perturbation method (CPM) while a control software implemented in LabVIEW obtains the desired heating rate adjusting the source bandwidth by means of a PID algorithm [15]. Being a technique that gives an overall precision of ± 1.3%, the dielectric values obtained for solar salt with a heating rate of 4.8 ºC/min and its thermos-physical properties are presented in the following table 1:

Table 1. Dielectric and thermo-physical properties of molten salt in the range of 285-565ºC.

Parameter	Value	Reference
Relative dielectric constant, ε'	0.01363×T+12.04	[5]
Dielectric loss, ε''	-0.001711×T+1.578	[5]
Thermal conductivity, k $(W/m \cdot {}^oC)$	$0.443+1.9\cdot10^{-4}$ ×T	[16]
Density, ρ (kg/m^3)	2090-0.636×T	[16]
Specific heat capacity, Cp $(J/kg \cdot {}^oC)$	1443+0.172×T	[16]
Absolute viscosity, μ $(mPa \cdot s)$	$22.714-0.120\times T+2.281\cdot10^{-4}\times T^2$ $-1.474\cdot10^{-7}\times T^3$	[16]

2.2 Model development

The first step is to generate the geometry including the waveguide, cavity and applicator tube. Figure 2 shows the two microwave heating systems modeled in this work.

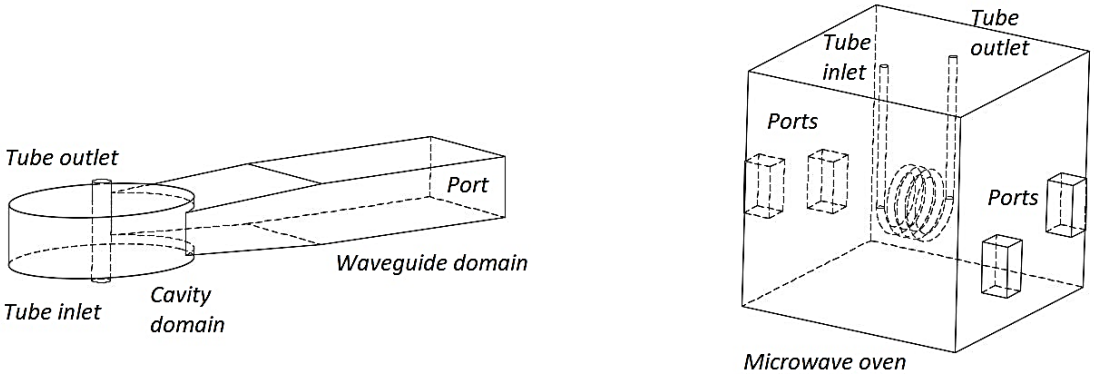

Figure 2. Schematic diagram of the continuous flow microwave heating system in elliptical single mode cavity (left) and in conventional microwave oven with helical tube (right).

The first model corresponds to a pilot scale TE_{10} mode specific to WR975 rectangular waveguide, perfect electric conductor walls in the waveguide and cavity, 915 MHz frequency, and 4.5 kW manufactured by Industrial Microwave Systems (IMS). The cavity is designed such that the fluid passing through the center of the tube made of PTFE, with the highest velocity, is exposed to high energy [17].

The second model consists of a rectangular cavity (0.5m x 0.5m x 0.5m), four WR430 rectangular waveguides, each port of 750 W and silicone tubes. The operating frequency is 2450 MHz. The tube, with an inner diameter of 0.016 m, minimally interferes with microwaves.

The mesh size of both models is based on the Nyquist criterion, equation (3), and based on this, for calculation accuracy, the maximum element size is set conservatively at 0.03 m in the waveguide and microwave cavity, and 0.004 m in the applicator tube for the first model, and 0.002 m in the helical tubing and 0.02 m in the waveguide and cavity for the second model.

$$S_{max} < \left[\frac{\lambda}{2} = \frac{c}{2f\sqrt{\varepsilon' \mu'}} \right] \quad (3)$$

Where S_{max} is the maximum grid element (m), λ is the free space length (m), f is the frequency of the wave (Hz), c is the speed of light in vacuum (m/s) and μ' is the relative permeability.

2.3 Governing equations

To determine the electric field distribution in a microwave cavity, Maxwell equations are solved as follows:

$$\nabla \times \left(\frac{1}{\mu_r} \nabla \times E \right) - \frac{\omega^2}{c} \left(\varepsilon' - i\varepsilon'' \right) E = 0 \quad (4)$$

Where E is the electric field intensity (V/m), ω is the angular wave frequency (rad/s), $\varepsilon_r = \varepsilon' - i\varepsilon''$ is relative permittivity and μ_r is relative permeability.

Total volumetric power generation (Q) due to microwave is calculated from the electric field intensity obtained:

$$Q = \sigma |E|^2 = 2\pi \varepsilon_0 \varepsilon'' f |E|^2 \quad (5)$$

Where σ is the electrical conductivity of the material (S/m) and ε_0 is the free space permittivity whose value is $8.854 \times 10^{-12}\ F/m$

The temperature distribution is obtained iteratively from electromagnetic calculations through the Fourier thermal balance equation from the total volumetric energy generation (Q):

$$\frac{\partial T}{\partial t} + \vec{u} \nabla T = \frac{k}{\rho C_p} \nabla^2 T + \frac{Q}{\rho C_p} \quad (6)$$

Likewise, the Navier-Stokes incompressible flow equation, equation (7), and the mass continuity equation, equation (8), are applied to obtain velocity profiles ($\vec{u}$) in the heated liquid:

$$\rho \frac{\partial \vec{u}}{\partial t} = -\nabla P + \mu \nabla^2 \vec{u} + \rho g \quad (7)$$

$$\nabla \cdot \vec{u} = 0 \quad (8)$$

Where ∇P is the pressure force (N/m^2) and g is the acceleration due to gravity (m/s^2)

2.4 Initial and boundary conditions

The following initial and boundary conditions have been considered:

- Electromagnetics is solved within the cavity and tube domain.
- The impedance boundary condition is used on external walls.
- Scattering boundary conditions for electromagnetics are applied at the inlet and outlet of the tube simulating an infinitely long pipe.
- Heat transfer and fluid flow is solved within the tube domain.

- The fluid is considered incompressible with an inlet temperature of 285ºC.
- No slip condition and thermal insulation are considered at the wall of the tube.

3. Results

3.1 Continuous flow microwave heating in elliptical single mode cavity

Solar salt heating in this single-mode cavity is studied at two different flow rates (1 l/min and 1.6 l/min). Another study comparing the electric field distribution, electromagnetic power generation density and temperature achieved in the solar salt when the tube is in the center of the cavity or displaced in the axial axis was performed.

3.1.1 Effects of the flow rate

In both cases – 1 l/min (0.021 m/s) and 1.6 l/min (0.034 m/s) – the electromagnetic distributions do not change. However, analyzing the average temperature in nine sections from inlet, it is possible to observe a lower temperature reached in the second case, as shown in figure 3.

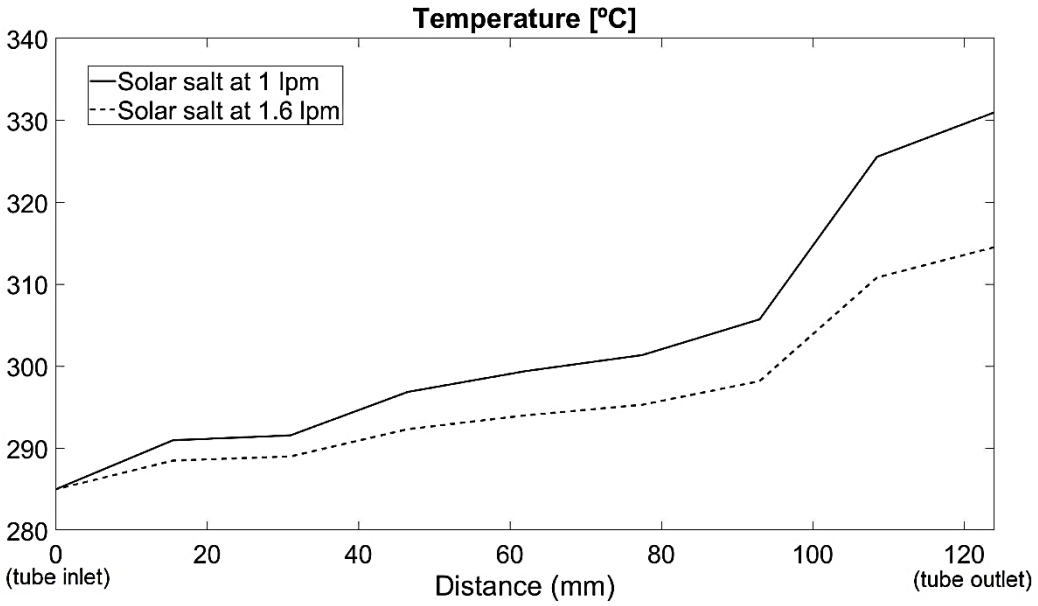

Figure 3. Cross-section average temperature for each flow rate.

The average temperature reached at the outlet of the cavity for a flow rate of 1 l/min is 330.98 ºC and for 1.6 l/min is 314.54 ºC. This leads to a difference in the power generated (Q) since the dielectric properties depend on temperature, table 1. So, the total absorbed power when solar salt flows at 1 l/min is 1839.6 W, while when it flows at 1.6 l/min is 1911.2 W. In conclusion, the residence time of the fluid inside the cavity is what determines the final temperature.

3.1.2 Effects of the position of the applicator tube

Based on the results obtained, figure 4, it can be observed how the position of the tube with the solar salt flowing, influences the electric field distribution within the cavity. This phenomenon is due to the variation in space of the relative permittivity, equation (4), which affects the electromagnetic power density, equation (5). As a result, the first case, which corresponds to the original design, has a high concentration throughout the wall with higher values of power density, while when the tube is displaced, the power gradient is located only on the side where the microwaves are incident with lower values of power density.

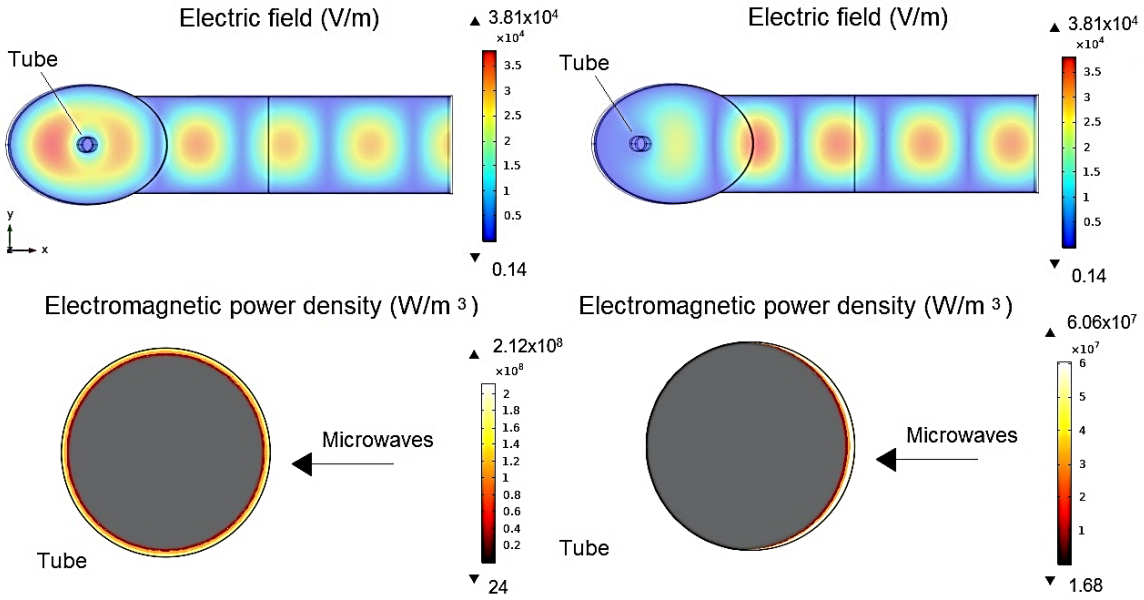

Figure 4. Electric field distribution xy plane, cross-section electromagnetic power for the tube at the center of the cavity (left) and displaced 83.36 mm in the axial axis (right).

This power density difference implies that while working with the applicator tube displaced around 8 cm from the center of the cavity, a barely 5 ºC increase in temperature at the tube outlet is achieved, while working with applicator tube in the center of the cavity, 9 times that increase (45 ºC) can be obtained at the same height, as shown in figure 5.

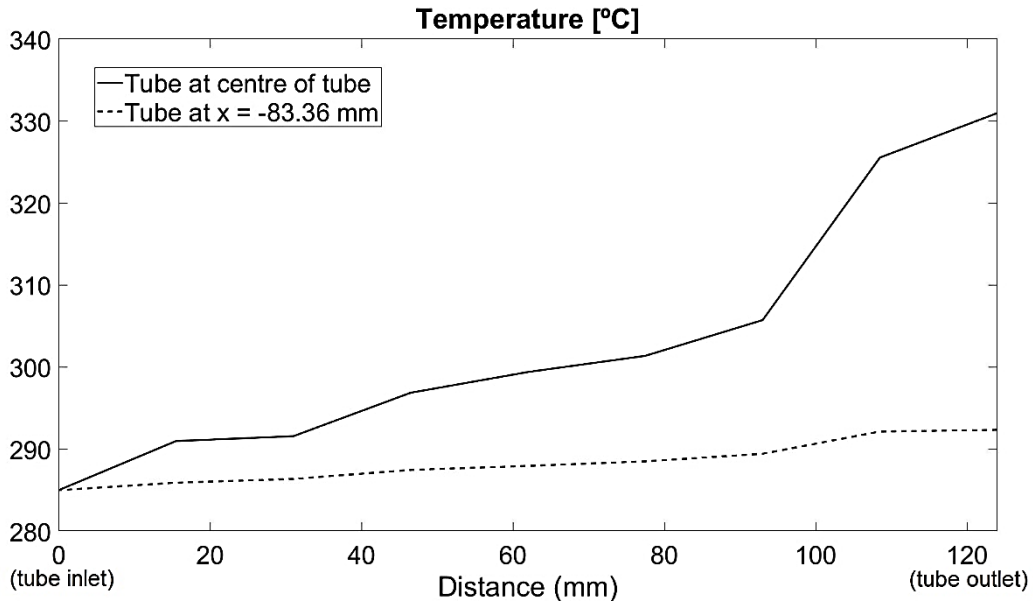

Figure 5. Cross-section average temperature for different positions of the applicator tube.

3.2 Continuous flow microwave heating in microwave oven with helical tubes

To overcome the non-uniform temperature distribution in multimode microwave ovens, sometimes a continuous flow system with a special geometry is used as proposed in [12].

Taking this idea, different cases with different number of turns (N = 3.5, 2.5 and 1.5) are simulated. The final average temperatures calculated are 371.86ºC, 353.21 ºC and 317.87ºC respectively. The temperature differences result obvious considering the longer path of the fluid inside the cavity. The following figure 6 shows the results for the case of N = 3.5.

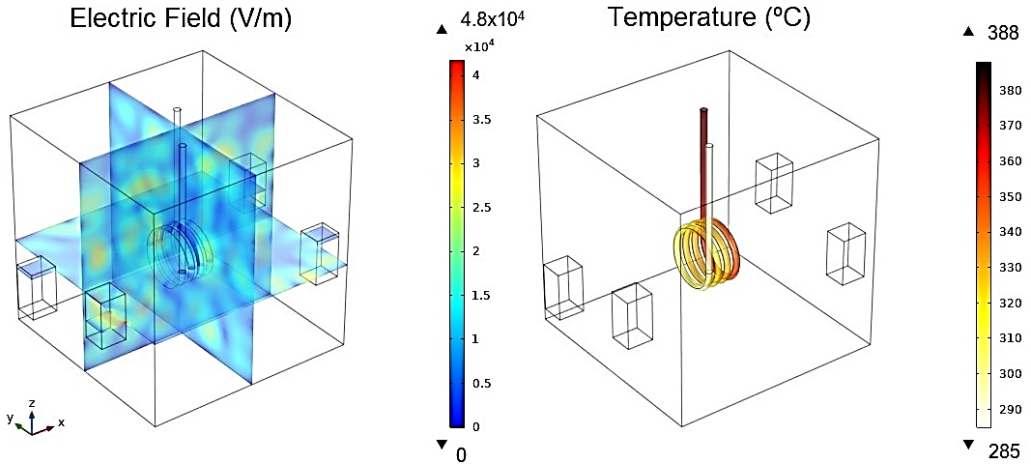

Figure 6. Electric field distribution inside the cavity and temperature distribution in the fluid.

4. Conclusion

This study highlights the differences in electric field distribution that a single-mode cavity can project with respect to a conventional microwave oven. However, there are techniques that allow a uniform temperature distribution such as continuous flow helical tubes.

Greater fluid permanence, either due to lower flow rate or special tube design, achieves higher temperatures. Furthermore, in the case of the elliptical cavity where a greater control of the process is possible, a different location of the applicator tube makes a big difference in the electric distribution, showing the great influence of the dielectric properties of the solar salt.

Data availability statement

The data needed to replicate the simulations are presented in the article itself. For more information, please contact the corresponding author.

Author contributions

Cristobal Valverde: Conceptualization, Software, Writing-original draft; Margarita M. Rodriguez-Garcia: Conceptualization, Supervision, Writing-review&editing; Esther Rojas: Conceptualization, Project administration, Writing-review&editing

Competing interests

The authors declare no competing interests.

References

1. M. Grolms. "Power-to-heat-to-power." Advanced science news. https://www.advancedsciencenews.com/power-to-heat-to-power/ (accessed Aug. 3, 2022).
2. L. Crespo. "The double role of CSP plants on the future Electrical Systems." Bloomberg NEF. https://about.bnef.com/blog/battery-pack-prices-cited-below-100-kwh-for-the-first-time-in-2020-while-market-average-sits-at-137-kwh/ (accessed Aug. 8, 2022).

3. O. Dumont, G. Francesco Frate, A. Pillai, S. Lecompte, M. De paepe, and V. Lemort, "Carnot battery technology: A state-of-the-art review," Journal of Energy Storage, vol. 32, p. 101756, 2020, doi: https://doi.org/10.1016/j.est.2020.101756.
4. Y. Han, Y. Sun, and J. Wu, "A low-cost and efficient solar/coal hybrid power generation mode: Integration of non-concentrating solar energy and air preheating process," Energy, vol. 235, p. 121367, 2021, doi: https://doi.org/10.1016/j.energy.2021.121367.
5. M. M. Rodriguez-García, R. Bayón, E. Alonso, and E. Rojas, "Experimental and Theoretical Investigation on Using Microwaves for Storing Electricity in a Thermal Energy Storage Medium," in SOLARPACES 2021: International Conference on Concentrating Solar Power and Chemical Energy Systems, 2021: AIP Publishing.
6. J. Zhu, A. V. Kuznetsov, and K. P. Sandeep, "Mathematical modeling of continuous flow microwave heating of liquids (effects of dielectric properties and design parameters)," International Journal of Thermal Sciences, vol. 46, no. 4, pp. 328-341, 2007, doi: https://doi.org/10.1016/j.ijthermalsci.2006.06.005.
7. S. Curet, F. Begnini, O. Rouaud, and L. Boillereaux, "Modeling Microwave Heating During Batch Processing of Liquid Sample in a Single Mode Cavity," 2015.
8. E. Rojas, M. Rodriguez-García, and C. Valverde. "Power-to-heat-to-power (P2H2P) usando microondas y sistemas comerciales de almacenamiento térmico de gran capacidad." madrimasd blogs. https://www.madrimasd.org/blogs/energiasalternativas/2022/05/23/135183 (accessed May 23, 2022).
9. J. Tang, "Unlocking Potentials of Microwaves for Food Safety and Quality," Journal of Food Science, vol. 80, no. 8, pp. E1776-E1793, 2015-08-01 2015, doi: https://doi.org/10.1111/1750-3841.12959.
10. C. Salazar-González, M. F. San Martín-González, A. López-Malo, and M. E. Sosa-Morales, "Recent Studies Related to Microwave Processing of Fluid Foods," Food and Bioprocess Technology, vol. 5, no. 1, pp. 31-46, 2012-01-01 2012, doi: https://doi.org/10.1007/s11947-011-0639-y.
11. G. S. J. Sturm, M. D. Verweij, T. v. Gerven, A. I. Stankiewicz, and G. D. Stefanidis, "On the effect of resonant microwave fields on temperature distribution in time and space," International Journal of Heat and Mass Transfer, vol. 55, no. 13, pp. 3800-3811, 2012, doi: https://doi.org/10.1016/j.ijheatmasstransfer.2012.02.065.
12. Y. Zhang et al., "Continuous flow microwave system with helical tubes for liquid food heating," Journal of Food Engineering, vol. 294, p. 110409, 2021, doi: https://doi.org/10.1016/j.jfoodeng.2020.110409.
13. D. Salvi, D. Boldor, J. Ortego, G. Aita, and C. Sabliov, "Numerical modeling of continuous flow microwave heating: A critical Comparison of COMSOL and ANSYS," The Journal of microwave power and electromagnetic energy : a publication of the International Microwave Power Institute, vol. 44, pp. 187-97, 01 2010, doi: https://doi.org/10.1080/08327823.2010.11689787.
14. P. A. Mello, J. S. Barin, and R. A. Guarnieri, "Chapter 2 - Microwave Heating," in Microwave-Assisted Sample Preparation for Trace Element Analysis, F. Érico Marlon de Moraes Flores Ed. Amsterdam: Elsevier, 2014, pp. 59-75. https://doi.org/10.1016/B978-0-444-59420-4.00002-7
15. J. M. Catala-Civera, A. J. Canos, P. Plaza-Gonzalez, J. D. Gutierrez, B. Garcia-Banos, and F. L. Penaranda-Foix, "Dynamic Measurement of Dielectric Properties of Materials at High Temperature During Microwave Heating in a Dual Mode Cylindrical Cavity," IEEE Transactions on Microwave Theory and Techniques, vol. 63, no. 9, pp. 2905-2914, 2015-09-01 2015, doi: https://doi.org/10.1109/tmtt.2015.2453263.
16. M.-M. Rodríguez-García, M. Herrador-Moreno, and E. Zarza Moya, "Lessons learnt during the design, construction and start-up phase of a molten salt testing facility," Applied Thermal Engineering, vol. 62, no. 2, pp. 520-528, 2014-01-01 2014, doi: https://doi.org/10.1016/j.applthermaleng.2013.09.040.
17. C. Sabliov, D. Salvi, and D. Boldor, "High Frequency Electromagnetism, Heat Transfer and Fluid Flow Coupling in ANSYS Multiphysics," The Journal of microwave power and electromagnetic energy : a publication of the International Microwave Power Institute, vol. 41, pp. 5-17, 02 2007, doi: https://doi.org/10.1080/08327823.2006.11688567.